Commun. Comput. Phys.
doi: 10.4208/cicp.OA-2023-0206

Vol. **35**, No. 1, pp. 160-180
January 2024

On the Monotonicity of Q^2 Spectral Element Method for Laplacian on Quasi-Uniform Rectangular Meshes

Logan J. Cross[1] and Xiangxiong Zhang[1,*]

[1] *Purdue University, 150 N. University Street, West Lafayette, IN 47907-2067, USA.*

Received 3 August 2023; Accepted (in revised version) 23 October 2023

Abstract. The monotonicity of discrete Laplacian implies discrete maximum principle, which in general does not hold for high order schemes. The Q^2 spectral element method has been proven monotone on a uniform rectangular mesh. In this paper we prove the monotonicity of the Q^2 spectral element method on quasi-uniform rectangular meshes under certain mesh constraints. In particular, we propose a relaxed Lorenz's condition for proving monotonicity.

AMS subject classifications: 65N30, 65N06, 65N12

Key words: Inverse positivity, discrete maximum principle, high order accuracy, monotonicity, discrete Laplacian, quasi uniform meshes, spectral element method.

1 Introduction

In many applications, monotone discrete Laplacian operators are desired and useful for ensuring stability such as discrete maximum principle or positivity-preserving of physically positive quantities [6, 10, 18, 21]. Let Δ_h denote the matrix representation of a discrete Laplacian operator, then it is called *monotone* if $(-\Delta_h)^{-1} \geq 0$, i.e., the inverse matrix $(-\Delta_h)^{-1}$ has nonnegative entries. In this paper, all inequalities for matrices are entrywise inequalities.

In the literature, the most important tool for proving monotonicity is via nonsingular M-matrices, which are inverse-positive matrices. See the Appendix for a convenient characterization of the M-matrices. The simplest second order accurate centered finite difference $u''(x_i) \approx \frac{u(x_{i-1})-2u(x_i)+u(x_{i+1})}{\Delta x^2}$ is monotone because the corresponding matrix $(-\Delta_h)^{-1}$ is an M-matrix thus inverse positive. Even though the linear finite element method forms an M-matrix on unstructured triangular meshes under a mild mesh constraint [24], in

*Corresponding author. *Email addresses:* `logancross68@gmail.com` (L. J. Cross), `zhan1966@purdue.edu` (X. Zhang)

general the discrete maximum principle is not true for high order finite element methods on unstructured meshes [9]. On the other hand, there exist a few high order accurate inverse positive schemes on structured meshes.

For solving a Poisson equation, provably monotone high order accurate schemes on structured meshes include the classical 9-point scheme [3, 7, 11] in which the stiffness matrix is an M-matrix. The classical 9-point scheme has the same stiffness matrix as fourth order accurate compact finite difference schemes [13], see the appendix in [16]. In [2,4], a fourth order accurate finite difference scheme was constructed and its stiffness matrix is a product of two M-matrices thus monotone. The Lagrangian P^2 finite element method on a regular triangular mesh [23] has a monotone stiffness matrix [19]. On an equilateral triangular mesh, the discrete maximum principle of P^2 element can also be proven [9]. Monotonicity was also proven for the Q^2 spectral element method on an uniform rectangular mesh for a variable coefficient Poisson equation under suitable mesh constraints [14]. The Q^k spectral element method is the continuous finite element method with Lagrangian Q^k basis implemented by $(k+1)$-point Gauss-Lobatto quadrature. The monotonicity of Q^3 spectral element method for Laplacian on uniform meshes was also proven in [8].

For proving inverse positivity, the main viable tool in the literature is to use M-matrices which are inverse positive. A convenient sufficient condition for verifying the M-matrix structure is to require that off-diagonal entries must be non-positive. Except the fourth order compact finite difference, all high order accurate schemes induce positive off-diagonal entries, destroying M-matrix structure, which is a major challenge of proving monotonicity. In [2] and [1], and also the appendix in [14], M-matrix factorizations of the form $(-\Delta_h)^{-1} = M_1 M_2$ were shown for special high order schemes but these M-matrix factorizations seem ad hoc and do not apply to other schemes or other equations. In [19], Lorenz proposed some matrix entry-wise inequality for ensuring a matrix to be a product of two M-matrices and applied it to P^2 finite element method on uniform regular triangular meshes.

In [14], Lorenz's condition was applied to Q^2 spectral element method on uniform rectangular meshes. Such a monotonicity result implies that the Q^2 spectral element method is bound-preserving or positivity-preserving for convection diffusion equations including the Allen-Cahn equation [21], the Keller-Segel equation [10], the Fokker-Planck equation [17], as well as the internal energy equation in compressible Navier-Stokes system [18]. On the other hand, all these results about Q^2 spectral element method are on uniform meshes. For both theoretical and practical interests, a natural question to ask is whether such a monotonicity result still holds on non-uniform meshes. The monotonicity of high order schemes on quasi-uniform meshes are preferred in many applications, e.g., [22].

The focus of this paper is to discuss Lorenz's condition for Q^2 spectral element method on quasi-uniform meshes. We discuss and derive sufficient mesh constraints to preserve monotonicity of Q^2 spectral element method on a quasi-uniform rectangular mesh. In general, the same discussion also applies to Lagrangian P^2 finite element method on a quasi-uniform regular triangular mesh, but there does not seem to be any advantage of using P^2.

For simplicity, we will focus only on Dirichlet boundary conditions. For Neumann boundary conditions, the discussion of monotonicity is very similar, e.g., see [10, 17] for discussion on Neumann boundaries.

The rest of the paper is organized as follows. In Section 2, we briefly review the Q^2 spectral element method and its equivalent finite difference form for the Poisson equation. In Section 3, we review the Lorenz's condition for proving monotonicity and propose a relaxed version of Lorenz's condition. Though we only focus on Q^2 spectral element method on quasi-uniform meshes for Laplacian in this paper, the proposed relaxed Lorenz's condition may also be used to derive monotonicity under more relaxed mesh constraints for Q^2 spectral element method solving variable coefficient problems such as those in [10, 14, 17]. In Section 4, we prove the monotonicity of Q^2 spectral element method on a quasi-uniform mesh by using the relaxed Lorenz's condition. Numerical tests of accuracy of the scheme and necessity of the mesh constraints for monotonicity are given in Section 5. Section 6 are concluding remarks.

2 Q^2 spectral element method

2.1 Finite element method with the simplest quadrature

Consider an elliptic equation on $\Omega=(0,1)\times(0,1)$ with Dirichlet boundary conditions:

$$\mathcal{L}u \equiv -\nabla\cdot(a\nabla u)+cu=f \quad \text{on } \Omega, \quad u=g \quad \text{on } \partial\Omega. \tag{2.1}$$

Assume there is a function $\bar{g}\in H^1(\Omega)$ as an extension of g so that $\bar{g}|_{\partial\Omega}=g$. The variational form of (2.1) is to find $\tilde{u}=u-\bar{g}\in H_0^1(\Omega)$ satisfying

$$\mathcal{A}(\tilde{u},v)=(f,v)-\mathcal{A}(\bar{g},v), \quad \forall v\in H_0^1(\Omega), \tag{2.2}$$

where $\mathcal{A}(u,v)=\iint_\Omega a\nabla u\cdot\nabla v dxdy+\iint_\Omega cuv dxdy$, $(f,v)=\iint_\Omega fv dxdy$.

Let h be quadrature point spacing of a rectangular mesh shown in Fig. 1 and $V_0^h\subseteq H_0^1(\Omega)$ be the continuous finite element space consisting of Q^2 polynomials, then the most convenient implementation of finite element method is to use the simple quadrature consisting of 3×3 Gauss-Lobatto quadrature rule for all the integrals, see Fig. 1 for Q^2 method. Such a numerical scheme can be defined as: find $u_h\in V_0^h$ satisfying

$$\mathcal{A}_h(u_h,v_h)=\langle f,v_h\rangle_h-\mathcal{A}_h(g_I,v_h), \quad \forall v_h\in V_0^h, \tag{2.3}$$

where $\mathcal{A}_h(u_h,v_h)$ and $\langle f,v_h\rangle_h$ denote using simple quadrature for integrals $\mathcal{A}(u_h,v_h)$ and (f,v_h) respectively, and g_I is the piecewise Q^2 Lagrangian interpolation polynomial at the quadrature points shown Fig. 1 of the following function:

$$g(x,y)=\begin{cases}0, & \text{if } (x,y)\in(0,1)\times(0,1),\\ g(x,y), & \text{if } (x,y)\in\partial\Omega.\end{cases}$$

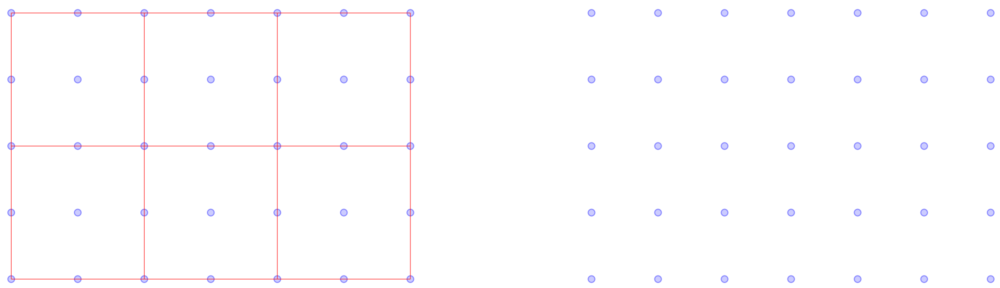

(a) The quadrature points and a finite element mesh (b) The corresponding finite difference grid

Figure 1: An illustration of Lagrangian Q^2 element and the 3×3 Gauss-Lobatto quadrature.

Then $\bar{u}_h = u_h + g_I$ is the numerical solution for the problem (2.1). Notice that (2.3) is not a straightforward approximation to (2.2) since $\bar{g}$ is never used. When the numerical solution is represented by a linear combination of Lagrangian interpolation polynomials at the grid points, it can be rewritten as a finite difference scheme. We can also call it a variational difference scheme since it is derived from the variational form.

2.2 The difference formulation

The scheme (2.3) with Lagrangian Q^2 basis can also be written as a finite difference scheme [15].

Consider a uniform grid (x_i,y_j) for a rectangular domain $[0,1]\times[0,1]$ where $x_i = ih$, $i=0,1,\cdots,n+1$ and $y_j = jh$, $j=0,1,\cdots,n+1$, $h=\frac{1}{n+1}$, where n must be odd. Let u_{ij} denote the numerical solution at (x_i,y_j). Let $\mathbf{u}$ denote an abstract vector consisting of u_{ij} for $i,j=1,2,\cdots,n$. Let $\bar{\mathbf{u}}$ denote an abstract vector consisting of u_{ij} for $i,j=0,1,2,\cdots,n,n+1$. Let $\bar{\mathbf{f}}$ denote an abstract vector consisting of f_{ij} for $i,j=1,2,\cdots,n$ and the boundary condition g at the boundary grid points. Then the matrix vector representation of (2.3) is $S\bar{\mathbf{u}} = M\mathbf{f}$ where S is the stiffness matrix and M is the lumped mass matrix. For convenience, after inverting the mass matrix, with the boundary conditions, the whole scheme can be represented in a matrix vector form $\bar{L}_h\bar{\mathbf{u}}=\bar{\mathbf{f}}$. For Laplacian $\mathcal{L}u=-\Delta u$, $\bar{L}_h\bar{\mathbf{u}}=\bar{\mathbf{f}}$ on a uniform mesh is given as

$$(\bar{L}_h\bar{\mathbf{u}})_{i,j} := \frac{-u_{i-1,j}-u_{i+1,j}+4u_{i,j}-u_{i,j+1}-u_{i+1,j}}{h^2} = f_{i,j}, \quad \text{if } (x_i,y_j) \text{ is a cell center,}$$

$$(\bar{L}_h\bar{\mathbf{u}})_{i,j} := \frac{-u_{i-1,j}+2u_{i,j}-u_{i+1,j}}{h^2} + \frac{u_{i,j-2}-8u_{i,j-1}+14u_{i,j}-8u_{i,j+1}+u_{i,j+2}}{4h^2} = f_{i,j},$$
$$\text{if } (x_i,y_j) \text{ is an edge center for an edge parallel to the } x\text{-axis,}$$

$$
\begin{aligned}
(\bar{L}_h\bar{\mathbf{u}})_{i,j}:=&\frac{u_{i-2,j}-8u_{i-1,j}+14u_{i,j}-8u_{i+1,j}+u_{i+2,j}}{4h^2}+\frac{-u_{i,j-1}+2u_{i,j}-u_{i,j+1}}{h^2}=f_{i,j},\\
&\text{if } (x_i,y_j) \text{ is an edge center for an edge parallel to the } y\text{-axis},\\
(\bar{L}_h\bar{\mathbf{u}})_{i,j}:=&\frac{u_{i-2,j}-8u_{i-1,j}+14u_{i,j}-8u_{i+1,j}+u_{i+2,j}}{4h^2}+\frac{u_{i,j-2}-8u_{i,j-1}+14u_{i,j}-8u_{i,j+1}+u_{i,j+2}}{4h^2}\\
&=f_{i,j}, \quad \text{if } (x_i,y_j) \text{ is a knot},\\
(\bar{L}_h\bar{\mathbf{u}})_{i,j}:=&u_{i,j}=g_{i,j} \quad \text{if } (x_i,y_j) \text{ is a boundary point.}
\end{aligned}
\tag{2.4}
$$

If ignoring the denominator h^2, then the stencil can be represented as:

$$
\text{cell center}\ \begin{array}{ccc} & -1 & \\ -1 & 4 & -1 \\ & -1 & \end{array}
\qquad
\text{knots}\ \begin{array}{ccccc} & & \frac{1}{4} & & \\ & & -2 & & \\ \frac{1}{4} & -2 & 7 & -2 & \frac{1}{4} \\ & & -2 & & \\ & & \frac{1}{4} & & \end{array}
$$

$$
\text{edge center (edge parallel to } y\text{-axis)}\ \begin{array}{ccccc} & & -1 & & \\ \frac{1}{4} & -2 & \frac{11}{2} & -2 & \frac{1}{4} \\ & & -1 & & \end{array}
$$

$$
\text{edge center (edge parallel to } x\text{-axis)}\quad \begin{array}{ccc} & \frac{1}{4} & \\ & -2 & \\ -1 & \frac{11}{2} & -1 \\ & -2 & \\ & \frac{1}{4} & \end{array}
$$

Remark 2.1. When regarded as a finite difference scheme, the scheme (2.3) is fourth order accurate in ℓ^2-norm for elliptic, parabolic, wave and Schrödinger equations [12,15].

3 Lorenz's condition for monotonicity

In this section, we first review the Lorenz's method for proving monotonicity [19], then present a relaxed Lorenz's condition. The definition of M-matrices is given in the appendix.

3.1 Discrete maximum principle

We first review how the monotonicity implies the discrete maximum principle for a boundary value problem. For a finite difference scheme, assume there are N grid points in the domain Ω and N^∂ boundary grid points on $\partial\Omega$. Define

$$
\mathbf{u}=\begin{pmatrix}u_1 & \cdots & u_N\end{pmatrix}^T,\quad \mathbf{u}^\partial=\begin{pmatrix}u_1^\partial & \cdots & u_{N^\partial}^\partial\end{pmatrix}^T,\quad \tilde{\mathbf{u}}=\begin{pmatrix}u_1 & \cdots & u_N & u_1^\partial & \cdots & u_{N^\partial}^\partial\end{pmatrix}^T.
$$

A finite difference scheme can be written as

$$\mathcal{L}_h(\tilde{\mathbf{u}})_i = \sum_{j=1}^{N} b_{ij} u_j + \sum_{j=1}^{N^\partial} b_{ij}^\partial u_j^\partial = f_i, \quad 1 \le i \le N,$$
$$u_i^\partial = g_i, \quad 1 \le i \le N^\partial.$$

The matrix form is

$$\tilde{L}_h \tilde{\mathbf{u}} = \tilde{\mathbf{f}}, \quad \tilde{L}_h = \begin{pmatrix} L_h & B^\partial \\ 0 & I \end{pmatrix}, \quad \tilde{\mathbf{u}} = \begin{pmatrix} \mathbf{u} \\ \mathbf{u}^\partial \end{pmatrix}, \quad \tilde{\mathbf{f}} = \begin{pmatrix} \mathbf{f} \\ \mathbf{g} \end{pmatrix}.$$

The discrete maximum principle is

$$\mathcal{L}_h(\tilde{\mathbf{u}})_i \le 0, \ 1 \le i \le N \implies \max_i u_i \le \max\{0, \max_i u_i^\partial\}, \tag{3.1}$$

which implies

$$\mathcal{L}_h(\tilde{\mathbf{u}})_i = 0, \ 1 \le i \le N \implies |u_i| \le \max_i |u_i^\partial|.$$

The following result was proven in [6]:

Theorem 3.1. *A finite difference operator $\mathcal{L}_h$ satisfies the discrete maximum principle* (3.1) *if $\tilde{L}_h^{-1} \ge 0$ and all row sums of $\tilde{L}_h$ are non-negative.*

With the same $\bar{L}_h$ as defined in the previous section, it suffices to have $\bar{L}_h^{-1} \ge 0$, see [14]:

Theorem 3.2. *If $\bar{L}_h^{-1} \ge 0$, then $\tilde{L}_h^{-1} \ge 0$ thus $L_h^{-1} \ge 0$. Moreover, if row sums of $\bar{L}_h$ are non-negative, then the finite difference operator $\mathcal{L}_h$ satisfies the discrete maximum principle.*

Let $\mathbf{1}$ be an abstract vector of the same shape as $\bar{\mathbf{u}}$ with all ones. For the Q^2 spectral element method, we have that $(\bar{L}_h \mathbf{1})_{i,j} = 1$ if $(x_i, y_j) \in \partial\Omega$ and $(\bar{L}_h \mathbf{1})_{i,j} = 0$ if $(x_i, y_j) \in \Omega$, which implies the row sums of $\bar{L}_h$ are non-negative. Thus from now on, we only need to discuss the monotonicity of the matrix $\bar{L}_h$.

3.2 Lorenz's sufficient condition for monotonicity

Definition 3.1. Let $\mathcal{N} = \{1, 2, \cdots, n\}$. For $\mathcal{N}_1, \mathcal{N}_2 \subset \mathcal{N}$, we say a matrix A of size $n \times n$ connects $\mathcal{N}_1$ with $\mathcal{N}_2$ if

$$\forall i_0 \in \mathcal{N}_1, \ \exists i_r \in \mathcal{N}_2, \ \exists i_1, \cdots, i_{r-1} \in \mathcal{N} \quad \text{s.t.} \quad a_{i_{k-1} i_k} \ne 0, \quad k = 1, \cdots, r. \tag{3.2}$$

If perceiving A as a directed graph adjacency matrix of vertices labeled by $\mathcal{N}$, then (3.2) simply means that there exists a directed path from any vertex in $\mathcal{N}_1$ to at least one vertex in $\mathcal{N}_2$. In particular, if $\mathcal{N}_1 = \emptyset$, then any matrix A connects $\mathcal{N}_1$ with $\mathcal{N}_2$.

Given a square matrix A and a column vector $\mathbf{x}$, we define

$$\mathcal{N}^0(A\mathbf{x})=\{i:(A\mathbf{x})_i=0\},\quad \mathcal{N}^+(A\mathbf{x})=\{i:(A\mathbf{x})_i>0\}.$$

Given a matrix $A=[a_{ij}]\in\mathbb{R}^{n\times n}$, define its diagonal, off-diagonal, positive and negative off-diagonal parts as $n\times n$ matrices A_d, A_a, A_a^+, A_a^-:

$$(A_d)_{ij}=\begin{cases}a_{ii}, & \text{if } i=j,\\ 0, & \text{if } i\neq j,\end{cases}\quad A_a=A-A_d,$$
$$(A_a^+)_{ij}=\begin{cases}a_{ij}, & \text{if } a_{ij}>0,\quad i\neq j,\\ 0, & \text{otherwise},\end{cases}\quad A_a^-=A_a-A_a^+.$$

The following two results were proven in [19]. See also [14] for a detailed proof.

Theorem 3.3. *If $A\le M_1M_2\cdots M_kL$ where $M_1,\cdots,M_k$ are nonsingular M-matrices and $L_a\le 0$, and there exists a nonzero vector $\mathbf{e}\ge 0$ such that $A\mathbf{e}\ge 0$ and one of the matrices $M_1,\cdots,M_k,L$ connects $\mathcal{N}^0(A\mathbf{e})$ with $\mathcal{N}^+(A\mathbf{e})$. Then $M_k^{-1}M_{k-1}^{-1}\cdots M_1^{-1}A$ is an M-matrix, thus A is a product of $k+1$ nonsingular M-matrices and $A^{-1}\ge 0$.*

Theorem 3.4 (Lorenz's condition)**.** *If A_a^- has a decomposition: $A_a^-=A^z+A^s=(a_{ij}^z)+(a_{ij}^s)$ with $A^s\le 0$ and $A^z\le 0$, such that*

$$A_d+A^z \text{ is a nonsingular M-matrix,} \tag{3.3a}$$

$$A_a^+\le A^zA_d^{-1}A^s \text{ or equivalently } \forall a_{ij}>0 \text{ with } i\neq j,\ a_{ij}\le\sum_{k=1}^n a_{ik}^z a_{kk}^{-1}a_{kj}^s, \tag{3.3b}$$

$$\exists\mathbf{e}\in\mathbb{R}^n\setminus\{\mathbf{0}\},\ \mathbf{e}\ge 0 \text{ with } A\mathbf{e}\ge 0 \text{ s.t. } A^z \text{ or } A^s \text{ connects } \mathcal{N}^0(A\mathbf{e}) \text{ with } \mathcal{N}^+(A\mathbf{e}). \tag{3.3c}$$

Then A is a product of two nonsingular M-matrices thus $A^{-1}\ge 0$.

Proposition 3.1. The matrix L in Theorem 3.3 must be an M-matrix.

Proof. Let $M^{-1}=M_k^{-1}M_{k-1}^{-1}\cdots M_1^{-1}$, following the proof of Theorem 7 in [14], then $M^{-1}A\mathbf{e}\ge cA\mathbf{e}$ for some positive number c. Then $A\mathbf{e}\ge 0\Rightarrow M^{-1}A\mathbf{e}\ge 0$. Now since $\mathbf{e}\ge 0$, $M^{-1}A\le L\Rightarrow 0\le(L-M^{-1}A)\mathbf{e}\Rightarrow M^{-1}A\mathbf{e}\le L\mathbf{e}$ thus $L\mathbf{e}\ge 0$.

Assume L connects $\mathcal{N}^0(A\mathbf{e})$ with $\mathcal{N}^+(A\mathbf{e})$. Since $M^{-1}A\mathbf{e}\le L\mathbf{e}$, $\mathcal{N}^0(L\mathbf{e})\subseteq\mathcal{N}^0(A\mathbf{e})$ and $\mathcal{N}^+(A\mathbf{e})\subseteq\mathcal{N}^+(L\mathbf{e})$, so L also connects $\mathcal{N}^0(L\mathbf{e})$ with $\mathcal{N}^+(L\mathbf{e})$.

Assume M_i connects $\mathcal{N}^0(A\mathbf{e})$ with $\mathcal{N}^+(A\mathbf{e})$, following the proof of Theorem 7 in [14], we have $M^{-1}A\mathbf{e}>0$. Now L trivially connects $\mathcal{N}^0(L\mathbf{e})$ with $\mathcal{N}^+(L\mathbf{e})$ since $L\mathbf{e}\ge M^{-1}A\mathbf{e}\Rightarrow L\mathbf{e}>0$ and $\mathcal{N}^0(L\mathbf{e})=\emptyset$.

Then Theorem 6 in [14] applies to show L is an M-matrix. $\square$

In practice, the condition (3.3c) can be difficult to verify. For variational difference schemes, the vector $\mathbf{e}$ can be taken as $\mathbf{1}$ consisting of all ones, then the condition (3.3c) can be simplified. The following theorem was proven in [14].

Theorem 3.5. *Let A denote the matrix representation of the variational difference scheme* (2.3) *with Q^2 basis solving $-\nabla\cdot(a\nabla)u+cu=f$. Assume A_a^- has a decomposition $A_a^-=A^z+A^s$ with $A^s\leq 0$ and $A^z\leq 0$. Then $A^{-1}\geq 0$ if the following are satisfied:*

1. *$(A_d+A^z)\mathbf{1}\neq\mathbf{0}$ and $(A_d+A^z)\mathbf{1}\geq 0$;*
2. *$A_a^+\leq A^zA_d^{-1}A^s$;*
3. *For $c(x,y)\geq 0$, either A^z or A^s has the same sparsity pattern as A_a^-. If $c(x,y)>0$, then this condition can be removed.*

3.3 A relaxed Lorenz's condition

In practice, both (3.3a) and (3.3b) impose mesh constraints for the Q^2 spectral element method on non-uniform meshes. The condition (3.3a) can be relaxed as the following:

Theorem 3.6 (A relaxed Lorenz's condition)**.** *If A_a^- has a decomposition: $A_a^-=A^z+A^s=(a_{ij}^z)+(a_{ij}^s)$ with $A^s\leq 0$ and $A^z\leq 0$, and there exists a diagonal matrix $A_{d^*}\geq A_d$ such that*

$$A_d^*+A^z \text{ is a nonsingular M-matrix,} \tag{3.4a}$$

$$A_a^+\leq A^zA_{d^*}^{-1}A^s, \tag{3.4b}$$

$$\exists\mathbf{e}\in\mathbb{R}^n\setminus\{\mathbf{0}\},\ \mathbf{e}\geq 0 \text{ with } A\mathbf{e}\geq 0 \text{ s.t. } A^z \text{ or } A^s \text{ connects } \mathcal{N}^0(A\mathbf{e}) \text{ with } \mathcal{N}^+(A\mathbf{e}). \tag{3.4c}$$

Then A is a product of two nonsingular M-matrices thus $A^{-1}\geq 0$.

Proof. It is straightforward that $A=A_d+A_a^++A^z+A^s\leq A_{d^*}+A^z+A^s+A^zA_{d^*}^{-1}A^s=(A_{d^*}+A^z)(I+A_{d^*}^{-1}A^s)$. By (3.4c), either $A_{d^*}+A^z$ or $I+A_{d^*}^{-1}A^s$ connects $\mathcal{N}^0(A\mathbf{e})$ with $\mathcal{N}^+(A\mathbf{e})$. By applying Theorem 3.3 for the case $k=1$, $M_1=A_{d^*}+A^z$ and $L=I+A_{d^*}^{-1}A^s$, we get $A^{-1}\geq 0$. □

Remark 3.1. Since $A_d\leq A_{d^*}$, only (3.4a) is more relaxed than (3.3a), and (3.4b) is more stringent than (3.3b). However, we will show in next section that it is possible to construct A_{d^*} such that (3.3b) and (3.4b) impose identical mesh constraints.

With Theorem A.1, combining Theorem 3.6 and Theorem 3.5, we have:

Theorem 3.7. *Let A denote the matrix representation of the variational difference scheme* (2.3) *with Q^2 basis solving $-\nabla\cdot(a\nabla)u+cu=f$. Assume A_a^- has a decomposition $A_a^-=A^z+A^s$ with $A^s\leq 0$ and $A^z\leq 0$ and there exists a diagonal matrix $A_{d^*}\geq A_d$. Then $A^{-1}\geq 0$ if the following are satisfied:*

1. *$(A_{d^*}+A^z)\mathbf{1}\neq\mathbf{0}$ and $(A_{d^*}+A^z)\mathbf{1}\geq 0$;*
2. *$A_a^+\leq A^zA_{d^*}^{-1}A^s$;*
3. *For $c(x,y)\geq 0$, either A^z or A^s has the same sparsity pattern as A_a^-. If $c(x,y)>0$, then this condition can be removed.*

4 Monotonicity of Q^2 spectral element method on quasi-uniform meshes

The Q^2 spectral element method has been proven monotone on a uniform mesh for Laplacian operator without any mesh constraints [14]. In this section, we will discuss its monotonicity for the Laplacian operator on quasi-uniform meshes. The discussion in this section can be easily extended to more general cases such as $\mathcal{L}u=-\Delta u+cu$ and Neumann boundary conditions. For simplicity, we only discuss the Laplacian case $\mathcal{L}u=-\Delta u$ and Dirichlet boundary conditions.

Consider a grid (x_i,y_j) $(i,j=0,1,\cdots,n+1)$ for a rectangular domain $[0,1]\times[0,1]$ where n must be odd and $i,j=0,n+1$ correspond to boundary points. Let u_{ij} denote the numerical solution at (x_i,y_j). Let $\bar{\mathbf{u}}$ denote an abstract vector consisting of u_{ij} for $i,j=0,1,2,\cdots,n,n+1$. Let $\bar{\mathbf{f}}$ denote an abstract vector consisting of f_{ij} for $i,j=1,2,\cdots,n$ and the boundary condition g at the boundary grid points. Then the matrix vector representation of (2.3) with Q^2 basis is $\bar{L}_h\bar{\mathbf{u}}=\bar{\mathbf{f}}$.

The focus of this section is to show $\bar{L}_h^{-1}\geq 0$ under suitable mesh constraints for quasi-uniform meshes. Moreover, it is straightforward to verify that $(\bar{L}_h\mathbf{1})_{i,j}=0$ for interior points (x_i,y_j) and $(\bar{L}_h\mathbf{1})_{i,j}=1$ for boundary points (x_i,y_j). Thus by Section 3.1, the scheme also satisfies the discrete maximum principle.

For simplicity, in the rest of this section we use A to denote the matrix $\bar{L}_h$ and let $\mathcal{A}$ be the linear operator corresponding to the matrix A. For convenience, we can also regard the abstract vector $\bar{\mathbf{u}}$ as a matrix of size $(n+2)\times(n+2)$. Then by our notation, the mapping $\mathcal{A}:\mathbb{R}^{(n+2)\times(n+2)}\rightarrow\mathbb{R}^{(n+2)\times(n+2)}$ is given as $\mathcal{A}(\bar{\mathbf{u}})_{i,j}:=(\bar{L}_h\bar{\mathbf{u}})_{i,j}$.

4.1 The scheme in two dimensions

For boundary points $(x_i,y_j)\in\partial\Omega$, the scheme is $\mathcal{A}(\bar{\mathbf{u}})_{i,j}:=u_{i,j}=g_{i,j}$. The scheme for interior grid points $(x_i,y_j)\in\Omega$ on a non-uniform mesh can be given on four distinct types of points shown in Fig. 2(b). For simplicity, from now on, we will use *edge center (2)* to denote an interior edge center for an edge parallel to the y-axis, and *edge center (3)* to denote an interior edge center for an edge parallel to the x-axis. The scheme at an interior grid point is given as $\mathcal{A}(\bar{\mathbf{u}})_{i,j}=f_{i,j}$ with

$$\mathcal{A}(\bar{\mathbf{u}})_{i,j}:=\frac{2h_a^2+2h_b^2}{h_a^2h_b^2}u_{i,j}-\left(\frac{1}{h_a^2}u_{i+1,j}+\frac{1}{h_a^2}u_{i-1,j}+\frac{1}{h_b^2}u_{i,j+1}+\frac{1}{h_b^2}u_{i,j-1}\right)$$
$$\text{if } (x_i,y_j) \text{ is a cell center;}$$

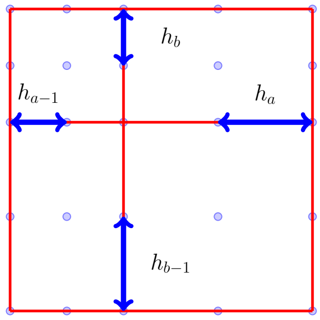

(a) Mesh length definitions for four adjacent Q^2 elements

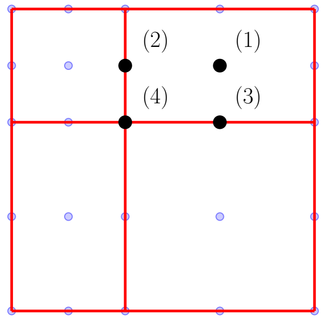

(b) The four distinct point types

Figure 2: A non-uniform mesh for Q^2 spectral element method. Each edge in a cell has length $2h$.

$$
\begin{aligned}
\mathcal{A}(\bar{\mathbf{u}})_{i,j} :=& \frac{7h_b^2+4h_ah_{a-1}}{2h_ah_{a-1}h_b^2}u_{i,j} - \frac{4}{h_a(h_a+h_{a-1})}u_{i+1,j} - \frac{4}{h_{a-1}(h_a+h_{a-1})}u_{i-1,j} \\
&-\frac{1}{h_b^2}u_{i,j+1} - \frac{1}{h_b^2}u_{i,j-1} + \frac{1}{2h_a(h_a+h_{a-1})}u_{i+2,j} + \frac{1}{2h_{a-1}(h_a+h_{a-1})}u_{i-2,j}, \\
&\text{if } (x_i,y_j) \text{ is edge center (2);} \\
\mathcal{A}(\bar{\mathbf{u}})_{i,j} :=& \frac{7h_a^2+4h_bh_{b-1}}{2h_bh_{b-1}h_a^2}u_{i,j} - \frac{4}{h_b(h_b+h_{b-1})}u_{i,j+1} - \frac{4}{h_{b-1}(h_b+h_{b-1})}u_{i,j-1} \\
&-\frac{1}{h_a^2}u_{i+1,j} - \frac{1}{h_a^2}u_{i-1,j} + \frac{1}{2h_b(h_b+h_{b-1})}u_{i,j+2} + \frac{1}{2h_{b-1}(h_b+h_{b-1})}u_{i,j-2}, \\
&\text{if } (x_i,y_j) \text{ is edge center (3);} \\
\mathcal{A}(\bar{\mathbf{u}})_{i,j} :=& \frac{7h_ah_{a-1}+7h_bh_{b-1}}{2h_ah_{a-1}h_bh_{b-1}}u_{i,j} - \left[\frac{4}{h_a(h_a+h_{a-1})}u_{i+1,j} + \frac{4}{h_{a-1}(h_a+h_{a-1})}u_{i-1,j}\right. \\
&\left.+\frac{4}{h_b(h_b+h_{b-1})}u_{i,j+1} + \frac{4}{h_{b-1}(h_b+h_{b-1})}u_{i,j-1}\right] + \frac{1}{2h_a(h_a+h_{a-1})}u_{i+2,j} \\
&+\frac{1}{2h_{a-1}(h_a+h_{a-1})}u_{i-2,j} + \frac{1}{2h_b(h_b+h_{b-1})}u_{i,j+2} + \frac{1}{2h_{b-1}(h_b+h_{b-1})}u_{i,j-2}, \\
&\text{if } (x_i,y_j) \text{ is an interior knot.}
\end{aligned} \tag{4.1}
$$

For a uniform mesh $h_a = h_{a-1} = h_b = h_{b-1} = h$, the scheme reduces to (2.4).

4.2 The decomposition of A_a^-

Next, by the same notations defined in Section 3.2, we will decompose the matrix $A = A_d + A_a^- + A_a^+$ and $A_a^- = A^z + A^s$ to verify Theorem 3.5. We will use $\mathcal{A}_a^-$, $\mathcal{A}_a^+$, $\mathcal{A}^z$ and $\mathcal{A}^s$ to denote linear operators for corresponding matrices. First, for the diagonal part we have

$$\mathcal{A}_d(\bar{\mathbf{u}})_{i,j}=u_{i,j},\quad \text{if } (x_i,y_j) \text{ is a boundary point;}$$
$$\mathcal{A}_d(\bar{\mathbf{u}})_{i,j}=\frac{2h_a^2+2h_b^2}{h_a^2h_b^2}u_{i,j},\quad \text{if } (x_i,y_j) \text{ is a cell center;}$$
$$\mathcal{A}_d(\bar{\mathbf{u}})_{i,j}=\frac{7h_b^2+4h_ah_{a-1}}{2h_ah_{a-1}h_b^2}u_{i,j},\quad \text{if } (x_i,y_j) \text{ is edge center (2);}$$
$$\mathcal{A}_d(\bar{\mathbf{u}})_{i,j}=\frac{7h_a^2+4h_bh_{b-1}}{2h_bh_{b-1}h_a^2}u_{i,j},\quad \text{if } (x_i,y_j) \text{ is edge center (3);}$$
$$\mathcal{A}_d(\bar{\mathbf{u}})_{i,j}=\frac{7h_bh_{b-1}+7h_ah_{a-1}}{2h_ah_{a-1}h_bh_{b-1}}u_{i,j},\quad \text{if } (x_i,y_j) \text{ is an interior knot.}$$

Notice that for a boundary point $(x_i,y_j)\in\partial\Omega$ we have $\mathcal{A}(\bar{\mathbf{u}})_{i,j}=\mathcal{A}_d(\bar{\mathbf{u}})_{i,j}=u_{i,j}$, thus for off-diagonal parts, we only need to look at the interior grid points. For positive off-diagonal entries, we have

$$\mathcal{A}_a^+(\bar{\mathbf{u}})_{i,j}=0,\quad \text{if } (x_i,y_j) \text{ is a cell center;}$$
$$\mathcal{A}_a^+(\bar{\mathbf{u}})_{i,j}=\frac{1}{2h_a(h_a+h_{a-1})}u_{i+2,j}+\frac{1}{2h_{a-1}(h_a+h_{a-1})}u_{i-2,j},\quad \text{edge center (2);}$$
$$\mathcal{A}_a^+(\bar{\mathbf{u}})_{i,j}=\frac{1}{2h_b(h_b+h_{b-1})}u_{i,j+2}+\frac{1}{2h_{b-1}(h_b+h_{b-1})}u_{i,j-2},\quad \text{edge center (3);}$$
$$\begin{aligned}\mathcal{A}_a^+(\bar{\mathbf{u}})_{i,j}=&\frac{1}{2h_a(h_a+h_{a-1})}u_{i+2,j}+\frac{1}{2h_{a-1}(h_a+h_{a-1})}u_{i-2,j}+\frac{1}{2h_b(h_b+h_{b-1})}u_{i,j+2}\\&+\frac{1}{2h_{b-1}(h_b+h_{b-1})}u_{i,j-2},\quad \text{if } (x_i,y_j) \text{ is an interior knot.}\end{aligned}$$

Then we perform a decomposition $A_a^-=A^z+A^s$, which depends on two constants $0<\epsilon_1\le 1$ and $0<\epsilon_2\le 1$.

$$\mathcal{A}^z(\bar{\mathbf{u}})_{i,j}=-\epsilon_1\left(\frac{1}{h_a^2}u_{i+1,j}+\frac{1}{h_a^2}u_{i-1,j}+\frac{1}{h_b^2}u_{i,j+1}+\frac{1}{h_b^2}u_{i,j-1}\right),\quad \text{if } (x_i,y_j) \text{ is a cell center;}$$
$$\begin{aligned}\mathcal{A}^z(\bar{\mathbf{u}})_{i,j}=&-\epsilon_1\left(\frac{1}{h_b^2}u_{i,j+1}+\frac{1}{h_b^2}u_{i,j-1}\right)-\epsilon_2\left[\frac{4}{h_a(h_a+h_{a-1})}u_{i+1,j}+\frac{4}{h_{a-1}(h_a+h_{a-1})}u_{i-1,j}\right],\\&\text{if } (x_i,y_j) \text{ is edge center (2);}\end{aligned}$$
$$\begin{aligned}\mathcal{A}^z(\bar{\mathbf{u}})_{i,j}=&-\epsilon_1\left(\frac{1}{h_a^2}u_{i+1,j}+\frac{1}{h_a^2}u_{i-1,j}\right)-\epsilon_2\left[\frac{4}{h_b(h_b+h_{b-1})}u_{i,j+1}+\frac{4}{h_{b-1}(h_b+h_{b-1})}u_{i,j-1}\right],\\&\text{if } (x_i,y_j) \text{ is edge center (3);}\end{aligned}$$

$$\mathcal{A}^z(\bar{\mathbf{u}})_{i,j} = -\epsilon_2 \left[\frac{4}{h_a(h_a+h_{a-1})} u_{i+1,j} + \frac{4}{h_{a-1}(h_a+h_{a-1})} u_{i-1,j} + \frac{4}{h_b(h_b+h_{b-1})} u_{i,j+1} + \frac{4}{h_{b-1}(h_b+h_{b-1})} u_{i,j-1} \right], \quad \text{if } (x_i,y_j) \text{ is an interior knot.}$$

Notice that A^z defined above has exactly the same sparsity pattern as A_a^- for $0<\epsilon_1\leq 1$ and $0<\epsilon_2\leq 1$. Let $A^s = A_a^- - A^z$ then $A^s \leq 0$.

4.3 Mesh constraints for $A^z A_d^{-1} A^s \geq A_a^+$

In order to verify $A^z A_d^{-1} A^s \geq A_a^+$, we only need to discuss nonzero entries in the output of $\mathcal{A}_a^+(\bar{\mathbf{u}})$ since $A^z A_d^{-1} A^s \geq 0$.

First consider the case that (x_i,y_j) is an interior knot. Fig. 3(a) shows the positive coefficients in the output of $\mathcal{A}_a^+(\bar{\mathbf{u}})_{ij}$ at a knot (x_i,y_j). Fig. 3(b) shows the stencil of $\mathcal{A}^z(\bar{\mathbf{u}})_{ij}$. Thus $\mathcal{A}^z(\bar{\mathbf{u}})$ acting as an operator on $[\mathcal{A}_d^{-1}\mathcal{A}^s](\bar{\mathbf{u}})$ at a knot is:

$$[\mathcal{A}^z\mathcal{A}_d^{-1}\mathcal{A}^s](\bar{\mathbf{u}})_{i,j} = -4\epsilon_2 \left[\frac{1}{h_a(h_{a-1}+h_a)} [\mathcal{A}_d^{-1}\mathcal{A}^s](\bar{\mathbf{u}})_{i+1,j} + \frac{1}{h_{a-1}(h_{a-1}+h_a)} [\mathcal{A}_d^{-1}\mathcal{A}^s](\bar{\mathbf{u}})_{i-1,j} + \frac{1}{h_b(h_{b-1}+h_b)} [\mathcal{A}_d^{-1}\mathcal{A}^s](\bar{\mathbf{u}})_{i,j+1} + \frac{1}{h_{b-1}(h_{b-1}+h_b)} [\mathcal{A}_d^{-1}\mathcal{A}^s](\bar{\mathbf{u}})_{i,j-1} \right].$$

In the expression above, the output of the operator $\mathcal{A}^z(\bar{\mathbf{u}})_{ij}$ are at interior edge centers as shown in Fig. 3(b). Hence $[\mathcal{A}_d^{-1}\mathcal{A}^s]$ will act on these edge centers with the mesh lengths corresponding to Fig. 2. Carefully considering the mesh lengths and operations of $\mathcal{A}_d^{-1}$

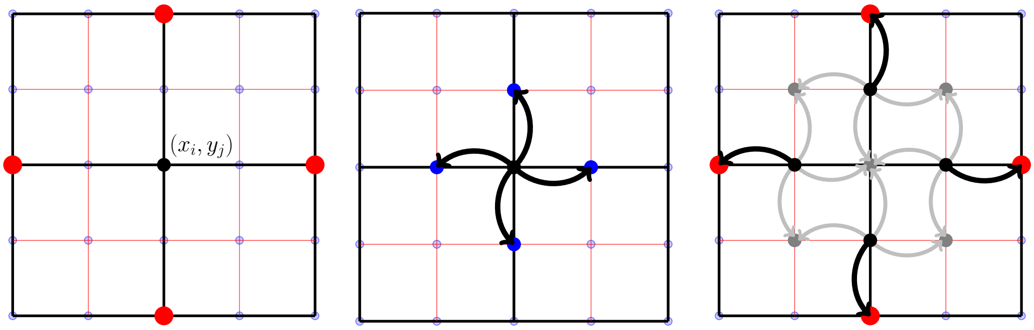

(a) Four red dots denote non-zero entry locations in $\mathcal{A}_a^+(\bar{\mathbf{u}})_{i,j}$

(b) Stencil of $\mathcal{A}^z(\bar{\mathbf{u}})_{i,j}$

(c) Stencil of $\mathcal{A}^z\mathcal{A}_d^{-1}\mathcal{A}^s(\bar{\mathbf{u}})_{i,j}$

Figure 3: Stencil of operators at an interior knot (x_i,y_j). The four red dots are the locations/entries where $\mathcal{A}_a^+(\bar{\mathbf{u}})_{i,j}$ are nonzero. Gray nodes in (c) represent positive entries that can be discarded for the purposes of verifying (3.4b). The mesh is illustrated as a uniform one only for simplicity.

at these points gives:

$$
\begin{aligned}
&[\mathcal{A}^z\mathcal{A}_d^{-1}\mathcal{A}^s](\bar{\mathbf{u}})_{i,j}\\
=&-4\epsilon_2\left[\frac{1}{h_a(h_{a-1}+h_a)}\frac{2h_bh_{b-1}h_a^2}{7h_a^2+4h_bh_{b-1}}\mathcal{A}^s(\bar{\mathbf{u}})_{i+1,j}\right.\\
&+\frac{1}{h_{a-1}(h_{a-1}+h_a)}\frac{2h_bh_{b-1}h_{a-1}^2}{7h_{a-1}^2+4h_bh_{b-1}}\mathcal{A}^s(\bar{\mathbf{u}})_{i-1,j}\\
&+\frac{1}{h_b(h_{b-1}+h_b)}\frac{2h_ah_{a-1}h_b^2}{7h_b^2+4h_ah_{a-1}}\mathcal{A}^s(\bar{\mathbf{u}})_{i,j+1}\\
&\left.+\frac{1}{h_{b-1}(h_{b-1}+h_b)}\frac{2h_ah_{a-1}h_{b-1}^2}{7h_{b-1}^2+4h_ah_{a-1}}\mathcal{A}^s(\bar{\mathbf{u}})_{i,j-1}\right],\quad \text{if } (x_i,y_j) \text{ is an interior knot.}
\end{aligned}
$$

Next consider the effect of $\mathcal{A}^s(\bar{\mathbf{u}})$ operator which has the same sparsity pattern as $\mathcal{A}^z(\bar{\mathbf{u}})$. Fig. 3(c) shows the stencil of $[\mathcal{A}^z\mathcal{A}_d^{-1}\mathcal{A}^s](\bar{\mathbf{u}})_{i,j}$ for an interior knot. Recall that $A^z\le 0$, $A^s\le 0$, and $A_d^{-1}\ge 0$, thus we have $A^zA_d^{-1}A^s\ge 0$. So we only need to compare the outputs of $[\mathcal{A}^z\mathcal{A}_d^{-1}\mathcal{A}^s](\bar{\mathbf{u}})_{i,j}$ and $\mathcal{A}_a^+(\bar{\mathbf{u}})_{i,j}$ at nonzero entries of $\mathcal{A}_a^+(\bar{\mathbf{u}})_{i,j}$, i.e., the four red dots in Fig. 3(a) and Fig. 3(c).

Thus we only need coefficients of $u_{i+2,j},u_{i-2,j},u_{i,j+2}$, and $u_{i,j-2}$ in the final expression of $[\mathcal{A}^z\mathcal{A}_d^{-1}\mathcal{A}^s](\mathbf{u})_{i,j}$, which are found to be

$$
\begin{aligned}
&u_{i+2,j}:\quad 4\epsilon_2(1-\epsilon_1)\tfrac{1}{h_a(h_{a-1}+h_a)}\tfrac{2h_bh_{b-1}h_a^2}{7h_a^2+4h_bh_{b-1}}\tfrac{1}{h_a^2};\\
&u_{i-2,j}:\quad 4\epsilon_2(1-\epsilon_1)\tfrac{1}{h_{a-1}(h_{a-1}+h_a)}\tfrac{2h_bh_{b-1}h_{a-1}^2}{7h_{a-1}^2+4h_bh_{b-1}}\tfrac{1}{h_{a-1}^2};\\
&u_{i,j+2}:\quad 4\epsilon_2(1-\epsilon_1)\tfrac{1}{h_b(h_{b-1}+h_b)}\tfrac{2h_ah_{a-1}h_b^2}{7h_b^2+4h_ah_{a-1}}\tfrac{1}{h_b^2};\\
&u_{i,j-2}:\quad 4\epsilon_2(1-\epsilon_1)\tfrac{1}{h_{b-1}(h_{b-1}+h_b)}\tfrac{2h_ah_{a-1}h_{b-1}^2}{7h_{b-1}^2+4h_ah_{a-1}}\tfrac{1}{h_{b-1}^2}.
\end{aligned}
$$

In order to maintain $A_a^+\le A^zA_d^{-1}A^s$, by comparing to the coefficients of $u_{i+2,j}$ for $\mathcal{A}_a^+(\bar{\mathbf{u}})$, we obtain a mesh constraint $4\epsilon_2(1-\epsilon_1)\frac{2h_bh_{b-1}}{7h_a^2+4h_bh_{b-1}}\ge\frac{1}{2}$. Similar constraints are obtained by comparing other coefficients at $u_{i,j\mp 2}$ and $u_{i-2,j}$. Define

$$\ell(\epsilon_1,\epsilon_2)=4\epsilon_2(1-\epsilon_1).$$

Then the following constraints are sufficient for $\mathcal{A}_a^+(\bar{\mathbf{u}})$ to be controlled by $\mathcal{A}^z\mathcal{A}_d^{-1}\mathcal{A}^s(\bar{\mathbf{u}})$ at an interior knot:

$$h_ah_{a-1}\ge\frac{7}{4\ell-4}\max\{h_b^2,h_{b-1}^2\},\quad h_bh_{b-1}\ge\frac{7}{4\ell-4}\max\{h_a^2,h_{a-1}^2\}. \tag{4.2a}$$

Second, we need to discuss the case when (x_i,y_j) is an interior edge center. Without loss of generality, assume (x_i,y_j) is an interior edge center of an edge parallel to the y-axis.

Then similar to the interior knot case, the output coefficients of $[\mathcal{A}^z\mathcal{A}_d^{-1}\mathcal{A}^s](\bar{\mathbf{u}})_{i,j}$ at the relevant non-zero entries of $\mathcal{A}_a^+(\bar{\mathbf{u}})_{i,j}$ are:

$$u_{i+2,j}: \quad 4\epsilon_2(1-\epsilon_1)\frac{1}{h_a(h_{a-1}+h_a)}\frac{h_a^2h_b^2}{2h_a^2+2h_b^2}\frac{1}{h_a^2};$$

$$u_{i-2,j}: \quad 4\epsilon_2(1-\epsilon_1)\frac{1}{h_{a-1}(h_{a-1}+h_a)}\frac{h_{a-1}^2h_b^2}{2h_{a-1}^2+2h_b^2}\frac{1}{h_{a-1}^2}.$$

By comparing with coefficients of $\mathcal{A}_a^+(\bar{\mathbf{u}})_{i,j}$, we get $\frac{h_b^2}{h_a^2+h_b^2}\geq\frac{1}{\ell}$, $\frac{h_b^2}{h_{a-1}^2+h_b^2}\geq\frac{1}{\ell}$. To ensure $\mathcal{A}_a^+(\bar{\mathbf{u}})$ is controlled by $\mathcal{A}^z\mathcal{A}_d^{-1}\mathcal{A}^s(\bar{\mathbf{u}})$ at edge centers, it suffices to have:

$$\min\{h_a,h_{a-1}\}\geq\sqrt{\frac{1}{\ell-1}}\max\{h_b,h_{b-1}\},\quad \min\{h_b,h_{b-1}\}\geq\sqrt{\frac{1}{\ell-1}}\max\{h_a,h_{a-1}\}. \tag{4.2b}$$

Note that $\mathcal{A}_a^+(\bar{\mathbf{u}})_{i,j}=0$ if (x_i,y_j) is a cell center. Since $\mathcal{A}^z\mathcal{A}_d^{-1}\mathcal{A}^s(\bar{\mathbf{u}})\geq 0$, there is no mesh constraint to enforce the inequality at cell centers.

4.4 Mesh constraints for A_d+A^z being an M-matrix

Let $\mathcal{B}=\mathcal{A}_d+\mathcal{A}^z$. Then $\mathcal{B}(\mathbf{1})_{i,j}=1$ for a boundary point (x_i,y_j). For interior points, we have:

$$\begin{aligned}
\mathcal{B}(\mathbf{1})_{i,j}&=-\epsilon_1\left(\frac{1}{h_a^2}+\frac{1}{h_a^2}+\frac{1}{h_b^2}+\frac{1}{h_b^2}\right)+\frac{2h_a^2+2h_b^2}{h_a^2h_b^2}=(1-\epsilon_1)\frac{2h_a^2+2h_b^2}{h_a^2h_b^2},\quad \text{cell center};\\
\mathcal{B}(\mathbf{1})_{i,j}&=-\epsilon_1\left(\frac{1}{h_b^2}+\frac{1}{h_b^2}\right)-\epsilon_2\left[\frac{4}{h_a(h_a+h_{a-1})}+\frac{4}{h_{a-1}(h_a+h_{a-1})}\right]+\frac{7h_b^2+4h_ah_{a-1}}{2h_ah_{a-1}h_b^2}\\
&=(1-\epsilon_1)\frac{2}{h_b^2}+\left(1-\frac{8}{7}\epsilon_2\right)\frac{7}{2h_ah_{a-1}},\quad \text{edge center (2)};\\
\mathcal{B}(\mathbf{1})_{i,j}&=-\epsilon_1\left(\frac{1}{h_a^2}+\frac{1}{h_a^2}\right)-\epsilon_2\left[\frac{4}{h_b(h_b+h_{b-1})}+\frac{4}{h_{b-1}(h_b+h_{b-1})}\right]+\frac{7h_a^2+4h_bh_{b-1}}{2h_bh_{b-1}h_a^2}\\
&=(1-\epsilon_1)\frac{2}{h_a^2}+\left(1-\frac{8}{7}\epsilon_2\right)\frac{7}{2h_bh_{b-1}},\quad \text{edge center (3)};\\
\mathcal{B}(\mathbf{1})_{i,j}&=-\epsilon_2\left[\frac{4}{h_a(h_a+h_{a-1})}+\frac{4}{h_{a-1}(h_a+h_{a-1})}+\frac{4}{h_b(h_b+h_{b-1})}+\frac{4}{h_{b-1}(h_b+h_{b-1})}\right]\\
&\quad+\frac{7h_bh_{b-1}+7h_ah_{a-1}}{2h_ah_{a-1}h_bh_{b-1}}=\left(1-\frac{8}{7}\epsilon_2\right)\frac{7h_bh_{b-1}+7h_ah_{a-1}}{2h_ah_{a-1}h_bh_{b-1}},\quad \text{interior knot}.
\end{aligned}$$

Notice that larger values of ℓ give better mesh constraints in (4.2). And we have $\sup_{0<\epsilon_1,\epsilon_2\leq 1}\ell(\epsilon_1,\epsilon_2)=\sup_{0<\epsilon_1,\epsilon_2\leq 1}4\epsilon_2(1-\epsilon_1)=4$. In order to apply Theorem A.1 for A_d+A^z be an M-matrix, we need $[\mathcal{A}_d+\mathcal{A}^z](\mathbf{1})\geq 0$. This is true if and only if $\epsilon_1\leq 1$ and $\epsilon_2\leq\frac{7}{8}$, which only give $\sup_{0<\epsilon_1\leq 1,0<\epsilon_2\leq\frac{7}{8}}\ell(\epsilon_1,\epsilon_2)=3.5$.

4.5 Improved mesh constraints by the relaxed Lorenz's condition

To get a better mesh constraint, the constraint on ϵ_2 can be relaxed so that the value of $\ell(\epsilon_1,\epsilon_2)$ can be improved. One observation from Section 4.3 is that the value of $\mathcal{A}_d(\bar{\mathbf{u}})_{i,j}$ for (x_i,y_j) being a knot is not used for verifying $A_a^+ \le A^z A_d^{-1} A^s$ (for both interior knots and edge centers). To this end, we define a new diagonal matrix A_{d^*}, which is different from A_d only at the interior knots.

$$
\begin{aligned}
&\mathcal{A}_{d^*}(\bar{\mathbf{u}})_{i,j} = u_{i,j} = \mathcal{A}_d(\bar{\mathbf{u}})_{i,j}, \quad \text{if } (x_i,y_j) \text{ is a boundary point;}\\
&\mathcal{A}_{d^*}(\bar{\mathbf{u}})_{i,j} = \frac{2h_a^2+2h_b^2}{h_a^2h_b^2}u_{i,j} = \mathcal{A}_d(\bar{\mathbf{u}})_{i,j}, \quad \text{if } (x_i,y_j) \text{ is a cell center;}\\
&\mathcal{A}_{d^*}(\bar{\mathbf{u}})_{i,j} = \frac{7h_b^2+4h_ah_{a-1}}{2h_ah_{a-1}h_b^2}u_{i,j} = \mathcal{A}_d(\bar{\mathbf{u}})_{i,j}, \quad \text{edge center (2);}\\
&\mathcal{A}_{d^*}(\bar{\mathbf{u}})_{i,j} = \frac{7h_a^2+4h_bh_{b-1}}{2h_bh_{b-1}h_a^2}u_{i,j} = \mathcal{A}_d(\bar{\mathbf{u}})_{i,j}, \quad \text{edge center (3);}\\
&\mathcal{A}_{d^*}(\bar{\mathbf{u}})_{i,j} = \frac{8h_bh_{b-1}+8h_ah_{a-1}}{2h_ah_{a-1}h_bh_{b-1}}u_{i,j} \ne \mathcal{A}_d(\bar{\mathbf{u}})_{i,j}, \quad \text{if } (x_i,y_j) \text{ is an interior knot.}
\end{aligned}
$$

Since the values of $\mathcal{A}_d(\bar{\mathbf{u}})_{i,j}$ for (x_i,y_j) being a knot is not involved in Section 4.3, the same discussion in Section 4.3 also holds for verifying $A_a^+ \le A^z A_{d^*}^{-1} A^s$. Namely, under mesh constraints (4.2), we also have $A_a^+ \le A^z A_{d^*}^{-1} A^s$.

Let $B^* = A_{d^*} + A^z$, then the row sums of B^* are:

$$
\begin{aligned}
&\mathcal{B}^*(\mathbf{1})_{i,j} = 1, \quad \text{if } (x_i,y_j) \text{ is a boundary point;}\\
&\mathcal{B}^*(\mathbf{1})_{i,j} = -\epsilon_1\left(\frac{1}{h_a^2}+\frac{1}{h_a^2}+\frac{1}{h_b^2}+\frac{1}{h_b^2}\right)+\frac{2h_a^2+2h_b^2}{h_a^2h_b^2} = (1-\epsilon_1)\frac{2h_a^2+2h_b^2}{h_a^2h_b^2}, \text{cell center;}\\
&\mathcal{B}^*(\mathbf{1})_{i,j} = -\epsilon_1\left(\frac{1}{h_b^2}+\frac{1}{h_b^2}\right)-\epsilon_2\left[\frac{4}{h_a(h_a+h_{a-1})}+\frac{4}{h_{a-1}(h_a+h_{a-1})}\right]+\frac{7h_b^2+4h_ah_{a-1}}{2h_ah_{a-1}h_b^2}\\
&\qquad = (1-\epsilon_1)\frac{2}{h_b^2}+\left(1-\frac{8}{7}\epsilon_2\right)\frac{7}{2h_ah_{a-1}}, \quad \text{edge center (2);}\\
&\mathcal{B}^*(\mathbf{1})_{i,j} = -\epsilon_1\left(\frac{1}{h_a^2}+\frac{1}{h_a^2}\right)-\epsilon_2\left[\frac{4}{h_b(h_b+h_{b-1})}+\frac{4}{h_{b-1}(h_b+h_{b-1})}\right]+\frac{7h_a^2+4h_bh_{b-1}}{2h_bh_{b-1}h_a^2}\\
&\qquad = (1-\epsilon_1)\frac{2}{h_a^2}+\left(1-\frac{8}{7}\epsilon_2\right)\frac{7}{2h_bh_{b-1}}, \quad \text{edge center (3);}\\
&\mathcal{B}^*(\mathbf{1})_{i,j} = -\epsilon_2\left[\frac{4}{h_a(h_a+h_{a-1})}+\frac{4}{h_{a-1}(h_a+h_{a-1})}+\frac{4}{h_b(h_b+h_{b-1})}+\frac{4}{h_{b-1}(h_b+h_{b-1})}\right]\\
&\qquad + \frac{8h_bh_{b-1}+8h_ah_{a-1}}{2h_ah_{a-1}h_bh_{b-1}} = (1-\epsilon_2)\frac{8h_bh_{b-1}+8h_ah_{a-1}}{2h_ah_{a-1}h_bh_{b-1}}, \quad \text{interior knot.}
\end{aligned}
$$

Now $[\mathcal{A}_{d^*}+\mathcal{A}^z](\mathbf{1})_{i,j} \ge 0$ at cell centers and knots is true if and only if $\epsilon_1 \le 1$ and $\epsilon_2 \le 1$.

Next, we will show that the mesh constraints (4.2) with $0<\epsilon_1\le\frac{1}{2}$ and $\epsilon_2=1$ are sufficient to ensure $[\mathcal{A}_{d^*}+\mathcal{A}^z](\mathbf{1})_{i,j}\ge 0$ at edge centers. We have $0<\epsilon_1\le\frac{1}{2}$, $\epsilon_2=1\Longrightarrow 2\le \ell<4\Longrightarrow \frac{7}{4\ell-4}\ge\frac{1}{\ell}$. The mesh constraints (4.2) imply that $h_ah_{a-1}\ge\frac{7}{4\ell-4}h_b^2\ge\frac{1}{\ell}h_b^2$, thus

$$(1-\epsilon_1)\frac{2}{h_b^2}+\left(1-\frac{8}{7}\epsilon_2\right)\frac{7}{2h_ah_{a-1}}=(1-\epsilon_1)\frac{2}{h_b^2}-\frac{1}{2}\frac{1}{h_ah_{a-1}}=\frac{1}{2}\left[\frac{\ell}{h_b^2}-\frac{1}{h_ah_{a-1}}\right]\ge 0.$$

Similarly, $(1-\epsilon_1)\frac{2}{h_a^2}+(1-\frac{8}{7}\epsilon_2)\frac{7}{2h_bh_{b-1}}\ge 0$ also holds.

Therefore, for constants $0<\epsilon_1\le\frac{1}{2}$ and $\epsilon_2=1$, we have $[\mathcal{A}_{d^*}+\mathcal{A}^z](\mathbf{1})\ge\mathbf{0}$. In particular, we have a larger ℓ compared to constraints from $\mathbf{A}_d$.

4.6 The main result

We have shown that for two constants $0<\epsilon_1\le\frac{1}{2}$ and $\epsilon_2=1$, under mesh constraints (4.2), the matrices A_{d^*}, A^z, A^s constructed above satisfy $(A_{d^*}+A^z)\mathbf{1}\ge\mathbf{0}$ and $A_a^+\le A^zA_{d^*}^{-1}A^s$.

For any fixed $\epsilon_1>0$ and $\epsilon_2=1$, A^z also has the same sparsity pattern as A. Thus if ℓ in (4.2) is replaced by $\sup_{0<\epsilon_1\le\frac{1}{2},\epsilon_2=1}\ell(\epsilon_1,\epsilon_2)=4$, Theorem 3.7 still applies to conclude that $A^{-1}\ge 0$.

Theorem 4.1. *The Q^2 spectral element method* (4.1) *has a monotone matrix $\bar{L}_h$ thus satisfies discrete maximum principle under the following mesh constraints:*

$$\begin{aligned}&h_ah_{a-1}\ge\frac{7}{12}\max\{h_b^2,h_{b-1}^2\},\quad h_bh_{b-1}\ge\frac{7}{12}\max\{h_a^2,h_{a-1}^2\},\\&\min\{h_a,h_{a-1}\}\ge\sqrt{\frac{1}{3}}\max\{h_b,h_{b-1}\},\quad \min\{h_b,h_{b-1}\}\ge\sqrt{\frac{1}{3}}\max\{h_a,h_{a-1}\},\end{aligned}\tag{4.3}$$

where h_a,h_{a-1} are mesh sizes for x-axis and h_b,h_{b-1} are mesh sizes for y-variable in four adjacent rectangular cells as shown in Fig. 2.

Remark 4.1. The following global constraint is sufficient to ensure (4.3):

$$\frac{25}{32}\le\frac{h_m}{h_n}\le\frac{32}{25},\tag{4.4}$$

where h_m and h_n are any two grid spacings in a non-uniform grid generated from a non-uniform rectangular mesh for Q^2 elements.

Remark 4.2. Though the mesh constraints above may not be sharp, similar constraints are necessary for monotonicity, as will be shown in numerical tests in the next section.

Remark 4.3. For Q^1 finite element method solving $-\Delta u=f$ to satisfy discrete maximum principle on non-uniform rectangular meshes [5], the mesh constraints are

$$h_ah_{a-1}\ge\frac{1}{2}\max\{h_b^2,h_{b-1}^2\}\quad h_bh_{b-1}\ge\frac{1}{2}\max\{h_a^2,h_{a-1}^2\}.\tag{4.5}$$

5 Numerical tests

5.1 Accuracy tests

We show some accuracy tests of the Q^2 spectral element method for solving $-\Delta u = f$ on a square $(0,1)\times(0,1)$ with Dirichlet boundary conditions. This scheme is fourth order accurate in ℓ^2-norm over quadrature points on uniform meshes [15]. On a quasi-uniform mesh, we test the error in ℓ^∞-norm to show that this is indeed a high order accurate scheme, which is at least third order accurate. We remark that Q^2 spectral element method as a finite difference scheme in ℓ^∞ norm is not fourth order accurate even on a uniform mesh, due to the singularity in Green's function in multiple dimensions, see numerical results in [15] and references therein.

Quasi-uniform meshes were generated by setting each pair of consecutive finite element cells along the axis to have a fixed ratio $\frac{h_k}{h_{k-1}} = 1.01$. The scheme is tested for the following very smooth solutions:

1. The Laplace equation $-\Delta u = 0$ with Dirichlet boundary conditions and $u(x,y) = \log((x+1)^2+(y+1)^2)+\sin(y)e^x$.

2. Poisson equation $-\Delta u = f$ with homogeneous Dirichlet boundary condition:
$$\begin{aligned} f(x,y) &= 13\pi^2\sin(3\pi y)\sin(2\pi x)+2y(1-y)+2x(1-x), \\ u(x,y) &= \sin(3\pi y)\sin(2\pi x)+xy(1-x)(1-y). \end{aligned} \tag{5.1}$$

3. Poisson equation $-\Delta u = f$ with nonhomogeneous Dirichlet boundary condition:
$$\begin{aligned} f &= 74\pi^2\cos(5\pi x)\cos(7\pi y)-8, \\ u &= \cos(5\pi x)\cos(7\pi y)+x^2+y^2. \end{aligned} \tag{5.2}$$

The errors of Q^2 spectral element method on quasi uniform rectangular meshes are listed in Table 1.

5.2 Necessity of mesh constraints

Even though the mesh constraints derived in the previous section are only sufficient conditions for monotonicity, in practice a mesh constraint is still necessary for the inverse positivity to hold. Consider a non-uniform Q^2 mesh with 5×5 cells on the domain $[0,1]\times[0,1]$, which has a 9×9 grid for the interior of the domain. Let the mesh on both axes be the same and let the four outer-most cells for each dimension be identical with length $2h$. Then the middle cell has size $2h'\times 2h'$ with $h' = \frac{1}{2}-2h$. Let the ratio h'/h increase gradually from $h'/h = 1$ (a uniform mesh) until the minimum value of the inverse of the matrix becomes negative. Increasing by values of 0.05, we obtain the first negative entry of $\bar{L}_h^{-1}$ at $h'/h = 5.35$ with $h = 0.0535$ and $h' = 0.2861$, and such a mesh is shown in Fig. 4(a). Fig. 4(b) shows how the smallest entry of $\bar{L}_h^{-1}$ decreases as h'/h increases.

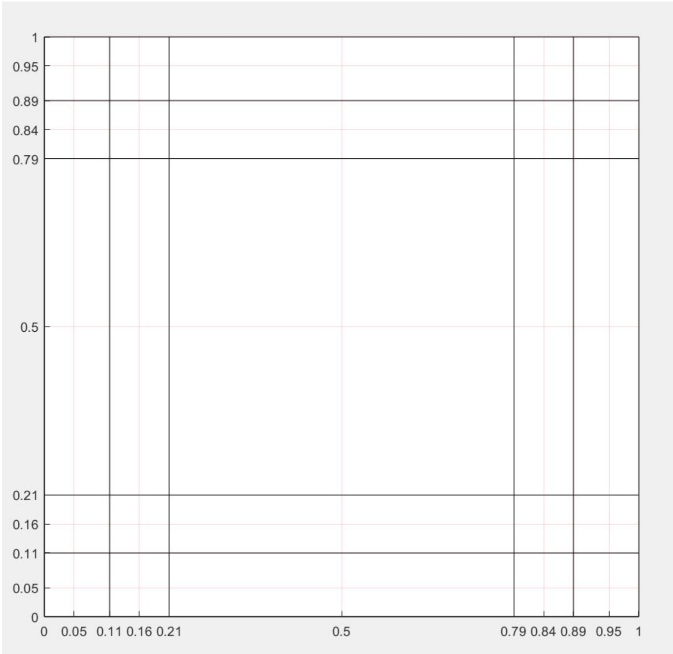

(a) A non-uniform mesh with 5×5 cells on which the Q^2 spectral element method is no longer monotone. The minimum value of $\bar{L}_h^{-1}$ is $-6.14E-8$.

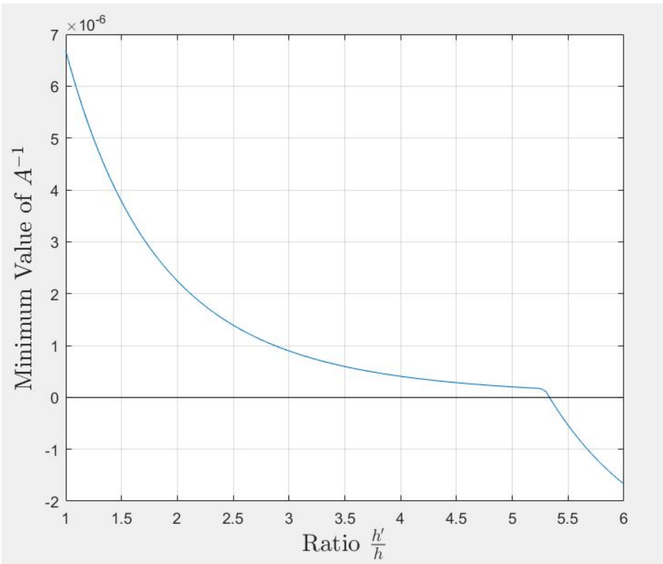

(b) A plot of the minimum value of $\bar{L}_h^{-1}$ as h'/h increases.

Figure 4: Necessity of mesh constraints for inverse positivity $\bar{L}_h^{-1}\geq 0$ where $\bar{L}_h$ is the matrix in Q^2 spectral element method on non-uniform meshes.

Table 1: Accuracy test on quasi-uniform meshes.

Finite Difference Grid	Ratio $\frac{h_i}{h_{i-1}}$	Q^2 spectral element method	
		l^∞ error	order
test on $-\Delta u = 0$			
7×7	1.01	2.66E-5	-
15×15	1.01	1.97E-6	3.74
31×31	1.01	1.54E-7	3.67
63×63	1.01	1.37E-8	3.49
test on (5.1)			
7×7	1.01	4.92E-2	-
15×15	1.01	3.19E-3	3.94
31×31	1.01	2.29E-4	3.79
63×63	1.01	1.80E-5	3.67
test on (5.2)			
7×7	1.01	1.20E-0	-
15×15	1.01	1.03E-1	3.54
31×31	1.01	9.10E-3	3.50
63×63	1.01	9.64E-4	3.23

6 Concluding remarks

By verifying a relaxed Lorenz's condition, we have discussed suitable mesh constraints, under which the Q^2 spectral element method on quasi-uniform meshes is monotone. Even though the derived mesh constraints may not be sharp, a similar constraint is necessary for the monotonicity to hold.

Acknowledgments

This research was supported by NSF DMS-1913120.

Appendix: M-matrices

Nonsingular M-matrices are inverse-positive matrices. There are many equivalent definitions or characterizations of M-matrices, see [20]. The following is a convenient sufficient but not necessary characterization of nonsingular M-matrices [14]:

Theorem A.1. *For a real square matrix A with positive diagonal entries and non-positive off-diagonal entries, A is a nonsingular M-matrix if all the row sums of A are non-negative and at least one row sum is positive.*

By condition K_{35} in [20], a sufficient and necessary characterization is:

Theorem A.2. *For a real square matrix A with positive diagonal entries and non-positive off-diagonal entries, A is a nonsingular M-matrix if and only if that there exists a positive diagonal matrix D such that AD has all positive row sums.*

Remark A.1. Non-negative row sum is not a necessary condition for M-matrices. For instance, the following matrix A is an M-matrix by Theorem A.2:

$$A = \begin{bmatrix} 10 & 0 & 0 \\ -10 & 2 & -10 \\ 0 & 0 & 10 \end{bmatrix}, \quad D = \begin{bmatrix} 0.1 & 0 & 0 \\ 0 & 2 & 0 \\ 0 & 0 & 0.1 \end{bmatrix}, \quad AD = \begin{bmatrix} 1 & 0 & 0 \\ -1 & 4 & -1 \\ 0 & 0 & 1 \end{bmatrix}.$$

References

[1] Erich Bohl and Jens Lorenz. Inverse monotonicity and difference schemes of higher order. A summary for two-point boundary value problems. *Aequationes Mathematicae*, 19(1):1–36, 1979.

[2] James H Bramble and Bert E Hubbard. New monotone type approximations for elliptic problems. *Mathematics of Computation*, 18(87):349–367, 1964.

[3] JH Bramble and BE Hubbard. On the formulation of finite difference analogues of the Dirichlet problem for Poisson's equation. *Numerische Mathematik*, 4(1):313–327, 1962.

[4] JH Bramble and BE Hubbard. On a finite difference analogue of an elliptic boundary problem which is neither diagonally dominant nor of non-negative type. *Journal of Mathematics and Physics*, 43(1-4):117–132, 1964.

[5] I Christie and C Hall. The maximum principle for bilinear elements. *International Journal for Numerical Methods in Engineering*, 20(3):549–553, 1984.

[6] Philippe G Ciarlet. Discrete maximum principle for finite-difference operators. *Aequationes Mathematicae*, 4(3):338–352, 1970.

[7] Lothar Collatz. *The Numerical Treatment of Differential Equations*. Springer-Verlag, Berlin, 1960.

[8] Logan J. Cross and Xiangxiong Zhang. On the monotonicity of Q^3 spectral element method for Laplacian. *arXiv:2010.07282*, 2023.

[9] Werner Höhn and Hans Detlef Mittelmann. Some remarks on the discrete maximum-principle for finite elements of higher order. *Computing*, 27(2):145–154, 1981.

[10] Jingwei Hu and Xiangxiong Zhang. Positivity-preserving and energy-dissipative finite difference schemes for the Fokker-Planck and Keller-Segel equations. *IMA Journal of Numerical Analysis*, 43(3):1450–1484, 2023.

[11] Vladimir Ivanovitch Krylov and Leonid Vital'evitch Kantorovitch. *Approximate Methods of Higher Analysis*. P. Noordhoff, 1958.

[12] Hao Li, Daniel Appelö, and Xiangxiong Zhang. Accuracy of spectral element method for wave, parabolic, and Schrödinger equations. *SIAM Journal on Numerical Analysis*, 60(1):339–363, 2022.

[13] Hao Li, Shusen Xie, and Xiangxiong Zhang. A high order accurate bound-preserving compact finite difference scheme for scalar convection diffusion equations. *SIAM Journal on Numerical Analysis*, 56(6):3308–3345, 2018.

[14] Hao Li and Xiangxiong Zhang. On the monotonicity and discrete maximum principle of the finite difference implementation of C^0-Q^2 finite element method. *Numerische Mathematik*, 145:437–472, 2020.
[15] Hao Li and Xiangxiong Zhang. Superconvergence of high order finite difference schemes based on variational formulation for elliptic equations. *Journal of Scientific Computing*, 82(2):36, 2020.
[16] Hao Li and Xiangxiong Zhang. A high order accurate bound-preserving compact finite difference scheme for two-dimensional incompressible flow. *Communications on Applied Mathematics and Computation*, pages 1–29, 2023.
[17] Chen Liu, Yuan Gao, and Xiangxiong Zhang. Structure preserving schemes for Fokker-Planck equations of irreversible processes. To appear in *Journal of Scientific Computing*, 98(1):4, 2024.
[18] Chen Liu and Xiangxiong Zhang. A positivity-preserving implicit-explicit scheme with high order polynomial basis for compressible Navier–Stokes equations. *Journal of Computational Physics*, 493:112496, 2023.
[19] Jens Lorenz. Zur inversmonotonie diskreter probleme. *Numerische Mathematik*, 27(2):227–238, 1977.
[20] Robert J Plemmons. M-matrix characterizations. I—-nonsingular M-matrices. *Linear Algebra and its Applications*, 18(2):175–188, 1977.
[21] Jie Shen and Xiangxiong Zhang. Discrete maximum principle of a high order finite difference scheme for a generalized Allen-Cahn equation. *Commun. Math. Sci.*, 20(5):1409–1436, 2022.
[22] M Sulman and T Nguyen. A positivity preserving moving mesh finite element method for the Keller–Segel chemotaxis model. *Journal of Scientific Computing*, 80(1):649–666, 2019.
[23] JR Whiteman. Lagrangian finite element and finite difference methods for poisson problems. In *Numerische Behandlung von Differentialgleichungen*, pages 331–355. Springer, 1975.
[24] Jinchao Xu and Ludmil Zikatanov. A monotone finite element scheme for convection-diffusion equations. *Mathematics of Computation*, 68(228):1429–1446, 1999.